Hindawi
International Journal of Antennas and Propagation
Volume 2021, Article ID 4206702, 8 pages
https://doi.org/10.1155/2021/4206702

Research Article

Broadband Dual-Polarized Multidipole Antenna for Base Station Applications

Yuxuan Huang ,[1,2] Zeqi Zhu,[1,2] Shuting Cai,[1,2] Xiaoming Xiong,[1,2] and Yuan Liu [1,2]

[1]*School of Automation, Guangdong University of Technology, Guangzhou 510006, China*
[2]*School of Microelectronics, Guangdong University of Technology, Guangzhou 510006, China*

Correspondence should be addressed to Yuan Liu; eeliuyuan@gdut.edu.cn

Received 18 April 2021; Revised 2 August 2021; Accepted 1 September 2021; Published 10 September 2021

Academic Editor: Giorgio Montisci

A wideband dual-polarized multidipole antenna for base station applications is proposed. It consists of a pair of large square-shaped loop dipoles and a pair of small rectangle loop dipoles as radiation elements. A pair of small rectangle loop dipoles is fed by T-shaped feed structure which is in the large square-shaped loop dipoles radiating arm so that the antenna generates an additional resonance and obtains a wider bandwidth. The proposed antenna was fabricated and measured, and the results show that the antenna achieves a wide impedance bandwidth of 63.7 % with VSWR<1.5 covering the frequency range from 1.55 to 3 GHz. A high isolation is better than 29 dB within the operating frequency bandwidth. Moreover, an average gain 8 dBi and a stable radiation pattern with 3 dB beamwidth of $69^{\circ} \pm 4^{\circ}$ at H-plane are obtained.

1. Introduction

Wireless communication systems have developed rapidly in recent years. To satisfy the demanding requirements in large cities, the desired antenna should be with good performance, such as wide impedance bandwidth, unidirectional radiation, stable gain, and stable radiation pattern [1]. Thus, dual-polarized antennas have become very popular in base station since they can reduce side effects of multipath fading and increase channel capacity [2, 3].

In order to achieve wide impedance bandwidth and small size, a number of crossed-dipoles antennas have been proposed for dual-polarized radiation. For different wideband feeding structures, Wen et al. [4] proposed a dipole antenna with Y-shaped feeding, which has a wide impedance bandwidth of 27.8% with VSWR < 1.5 (1.7–2.25 GHz). As reported in [5], two pairs of circular slotted square dipoles are fed by two fan-shaped microstrip lines to obtain a bandwidth of 48.2% with VSWR < 1.4 (1.62–2.68 GHz). An antenna has been fed by four capacitive F-probes with two-layer patches in [6], which introduces a balanced feeding structure to realize high isolation and low cross polarization. Huang et al. [7] proposed the ME dipole antenna with C-shaped stubs to filter the unwanted frequency band, which has a bandwidth of 52.6% for VSWR < 1.5 and a port-to-port isolation higher than 25.4 dB. Moreover, by using balun structure [8–10] and adding parasitic elements (such as folded metallic plate [11], loop ring [1,12], and fan-shaped parasitic patches [13]), the bandwidth can be effectively increased. However, the proposed crossed-dipoles antennas mostly suffer from large dimension complicated structure and a narrow impedance bandwidth that are still less than 55 %.

In this paper, a broadband dual-polarized multidipole antenna for 2 G/3 G/LTE base station is proposed. A small T-shaped feed structure is designed in the each large square-shaped dipole. Thus, the loaded small rectangular loop dipoles are excited, and a new resonance is generated at high frequency. The proposed antenna obtains a wide impedance bandwidth, a stable radiation pattern, and a stable antenna gain in the desired band (1550–3000 GHz), which are sufficient to cover all the frequency bands of 2 G/3 G/LTE communication systems. In addition, it can be easily fabricated on a large scale due to its simple and compact planar structure.

2. Antenna Configuration

Figure 1 shows the configuration of the proposed antenna. This antenna consists of a square ground plane used as reflector with a size of 130 mm × 130 mm, two Y-shaped feeding lines, a pair of large cross square-shaped loop radiator dipoles, a pair of small rectangle loop radiation dipoles, and two coaxial cable feeds. As shown in Figure 1, the small loop radiation dipoles and Y-shaped feeding lines are printed on the top face of the FR4 substrate with a thickness $h0 = 0.8$ mm, a dielectric constant of $\varepsilon_r = 4.4$, and a tan $\delta = 0.02$. To avoid overlap, one of the feeding structures is printed on the bottom of substrate and connected with the remaining part of the feeding lines on the top by two shorting copper pins via hole [14]. Meanwhile, the large loop dipoles are printed on the bottom of the substrate and fed by two Y-shaped feeding lines. The inner conductor of each coaxial cable is connected to a feeding structure, while its outer conductor is soldered to one arm. To achieve a unidirectional radiation, the outer conductor of each coaxial cable is also connected with the reflector that is $h = 35$ mm (about $0.25\lambda_0$) away from the substrate. The proposed antenna is simulated by Ansys HFSS, and the optimized parameters are listed in Table 1.

3. Antenna Design

3.1. Design of Antenna Element. Figure 2 shows the evolution of the proposed antenna. To study the influence of parasitic elements on antenna bandwidth and gain, the simulated $|S_{11}|$ and gain of Ant. 1, Ant. 2, and Ant. 3 are shown in Figures 3 and 4. It can been seen that based on the antenna structure with two Y-shaped feeding lines (Figure 2(a)), as adding four small squares in the corner of the large loop dipoles, the working frequency bandwidth broadens and the gain has been slightly improved [2]. Ant. 2 with a small square has two resonances which are excited at 1.65 GHz and 2.4 GHz. The impedance bandwidth is about 45% range from 1.6 GHz to 2.55 GHz for VSWR < 1.5. At the same time, compared with Ant. 1, the gain of the Ant. 2 has been slightly improved. Moreover, by adding a small T-shaped feed line in the radiating arm of each large loop dipoles, the electromagnetic coupling between the large loop dipoles and the small loop dipoles is generated at high frequencies. Therefore, a new resonance is generated at 2.95 GHz, the impedance bandwidth of the proposed antenna with the small loop dipoles is about 63.7% range from 1.55 GHz to 3 GHz for VSWR < 1.5, and the average gain is about 8.5 dBi. Compared with Ant. 1 and Ant. 2, the new dipole antenna shows a significant improvement in impedance bandwidth performance. The loaded small loop dipoles are excited, and the proposed antenna achieves a wider impedance bandwidth and higher gain than Ant. 1 and Ant. 2.

The current distributions of the proposed antenna with the small loop dipoles are shown in Figure 5 at three resonant frequencies (1.65 GHz, 2.45 GHz, and 2.95 GHz). Due to the symmetry of the feeding structure, it is assumed that only one port is excited for simplicity. When one loop dipole is driven, the other loop dipole can be used as parasitic elements. As shown in Figures 4(a) and 4(b), the antenna can achieve the polarization of +45 and the currents are observed mainly on the large dipoles. Thus, the resonances at 1.65 GHz and 2.45 GHz are dominated by the large loop dipoles. As shown in Figure 4(c), obviously currents are both observed on the large dipoles and small loop dipoles although the current direction of these two parts is opposite. As a result, the strong electromagnetic coupling between large loop dipoles and small loop dipoles changes the resonant mode in high frequency bands.

3.2. Parameter Analysis. To investigate the effects of design parameters on the VSWR, only one parameter is optimized while the others are fixed. Figure 6 shows the effects of W1, L7, O2, and O3 on the VSWR and S12.

W1 is the distance between two large loop dipoles. As shown in Figure 6(a), with the increment of W1, the impedance bandwidth increases gradually and the isolation between the two ports becomes worse. However, the value of VSWR when $W1 = 1.8$ mm is larger than that when $W1 = 1.2$ mm. By considering of bandwidth and impedance matching, $W1 = 1.2$ mm is selected.

As mentioned above, small dipoles lead to another resonance mode and the increment of bandwidth. Therefore, it is necessary to optimize the parameter (L7) of the small dipoles. Figure 6(b) presents the effect of L7 on VSWR. As shown in Figure 6(b), the third resonance point shifts to the lower frequency with the increment of L7. In addition, the performance of VSWR improves with the increment of L7. By considering bandwidth and impedance matching, $L7 = 10$ mm is selected.

O2 and O3 are the width and length of the T-shaped structure, respectively. As shown in Figures 6(c) and 6(d), the effects of O2 and O3 on VSWR and S21 are also analysed. With the increment of O2 and O3, isolation performance and impedance matching performance become better. Therefore, the value of O2 and O3 is about 1.2 mm and 2.75 mm, respectively.

3.3. Measured Results. Based on the above designed parameters, a prototype of the proposed antenna has been fabricated, as shown in Figure 7.

The measured results of the two ports are nearly the same due to the symmetry of the antenna. Thus, only the radiation patterns of port 1 are given. The measured and simulated differential gain and VSWR are shown in Figure 8. The corresponding values VSWR<1.5 can cover wide frequency bands of 1.55~3 GHz and 1.55~2.95 GHz for simulated and measure results, respectively. Good agreements are achieved between measured and simulated results. The slight deviation is induced by the manufacturing tolerances and measurement errors.

The average gain over the operating frequency band is about 8 dBi, and the maximum gain is about 8.7 dBi at 2.5 GHz. As shown in Figure 9, the measured isolation between the 1 port to 2 port is more than 29 dB, but the simulated result is a little higher than measured. The

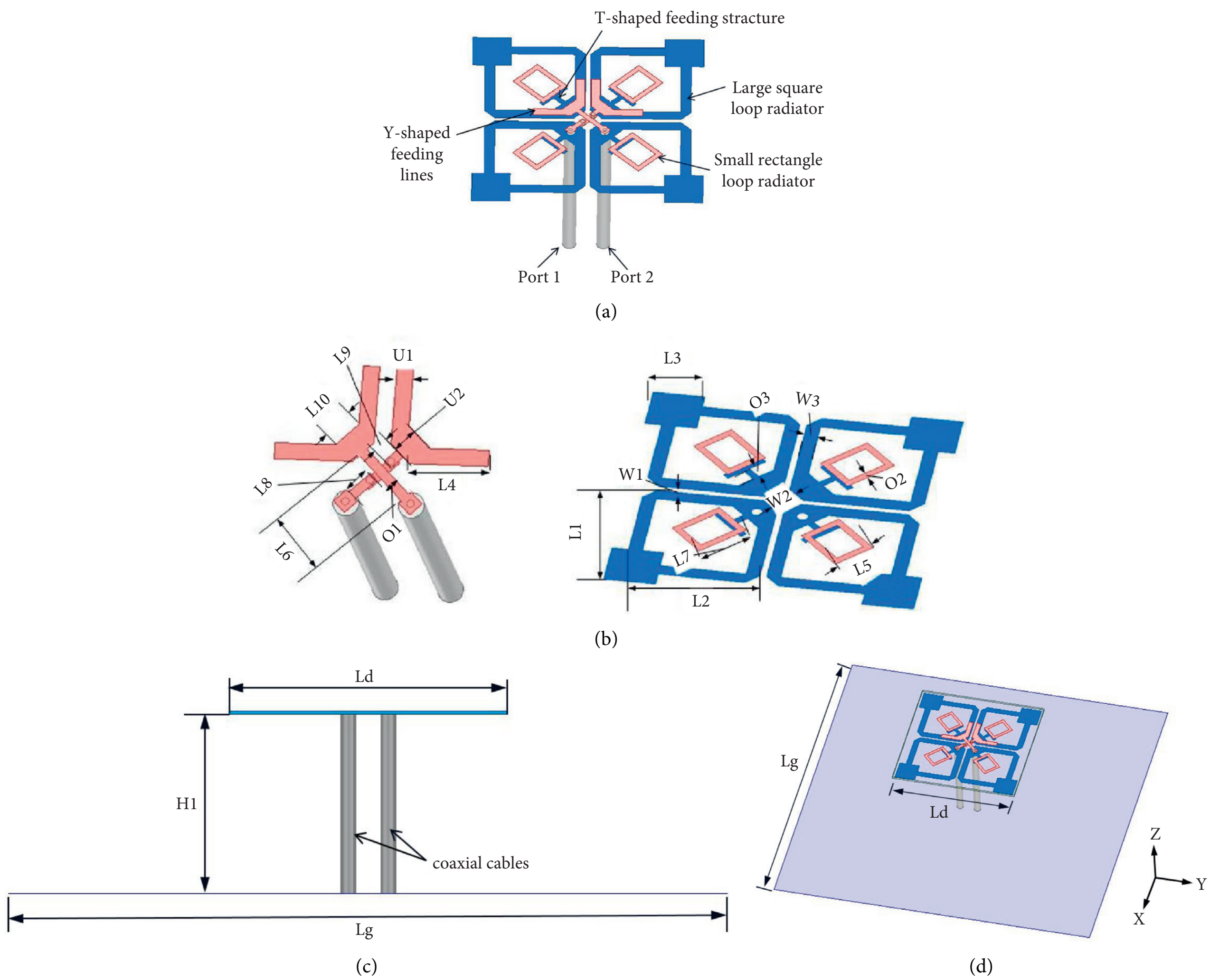

FIGURE 1: Geometry of the proposed antenna: (a) antenna element; (b) feeding structure and dipoles; (c) side view; (d) 3D view.

TABLE 1: Design parameters of the proposed antenna.

Parameter	Value (mm)
Lg	130
Ld	56
H1	35
L1	23.5
L2	18.7
L3	9
L4	12
L5	8
L6	9.8
L7	10
L8	2.53
L9	2.2
L10	6
O1	1.2
O2	1.2
O3	2.75
U1	2
U2	3
WI	1.2
W2	5.5

difference between simulated and measured port-to-port isolation results from the fabrication error, feeding mechanism, and the effect of not adding the SMA ports during the simulation. In addition, the average efficiency of 95% in the operating band is realized. Figure 10 presents the simulated and measured normalized radiation patterns of the proposed antenna at three frequencies (1.65 GHz, 2.45 GHz, and 2.95 GHz). The simulated and measured co-polarization patterns are in good agreement. Except for the measured results at 2.95 GHz, the cross polarization is larger than 20 dB in the main beam direction. This issue may be due to the radiation from the currents flowing on the small rectangle loop dipoles. A stable radiation pattern with HPBW of 68 ± 3 at XZ-plane and 69 ± 4 at YZ-plane is achieved in the whole working frequency band.

A comparison between the proposed antenna and the reported designs is listed in Table 2. It can be seen from the table that the proposed antenna has a widest usable impedance bandwidth and better port isolation without complicated structure when compared with those antennas.

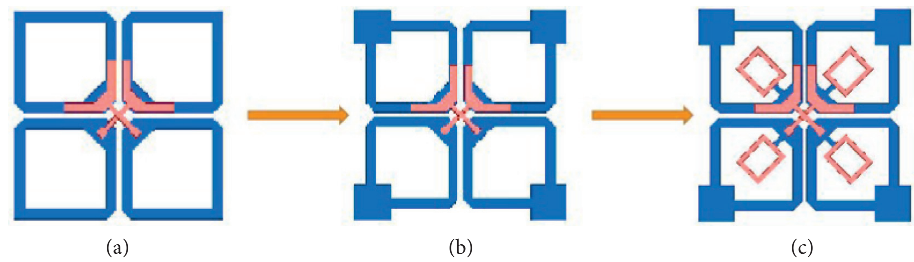

Figure 2: Evolution of the proposed antenna.

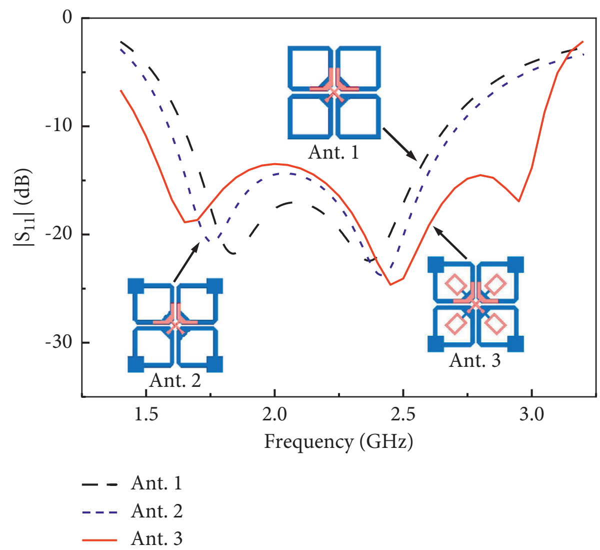

Figure 3: Simulated $|S_{11}|$ of three types of dipole antenna.

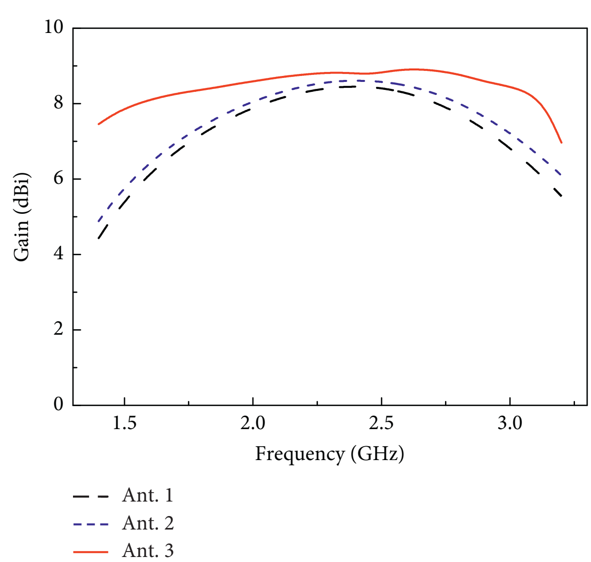

Figure 4: Simulated gain of three types of dipole antenna.

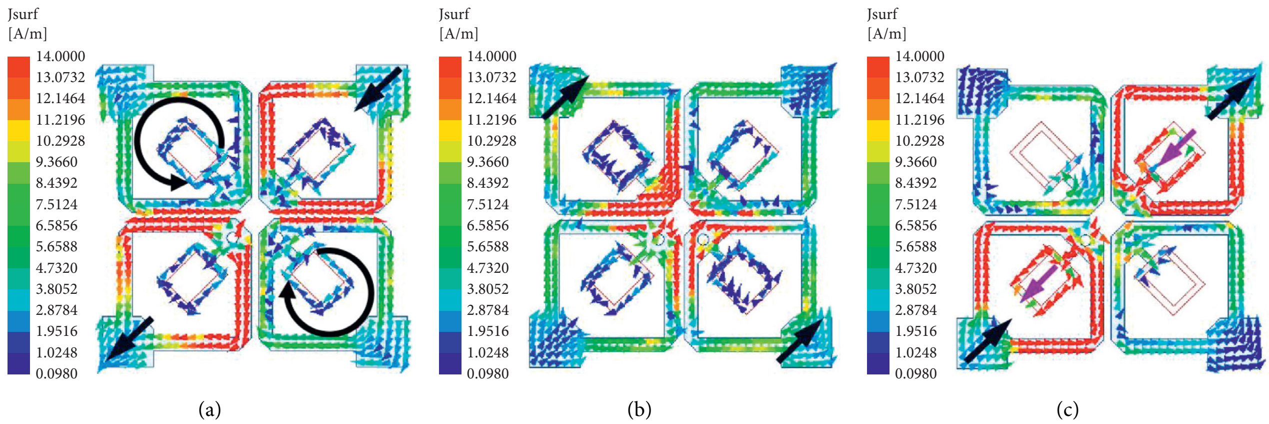

Figure 5: The current distributions of the antenna at (a) 1.65 GHz; (b) 2.65 GHz; (c) 2.95 GHz.

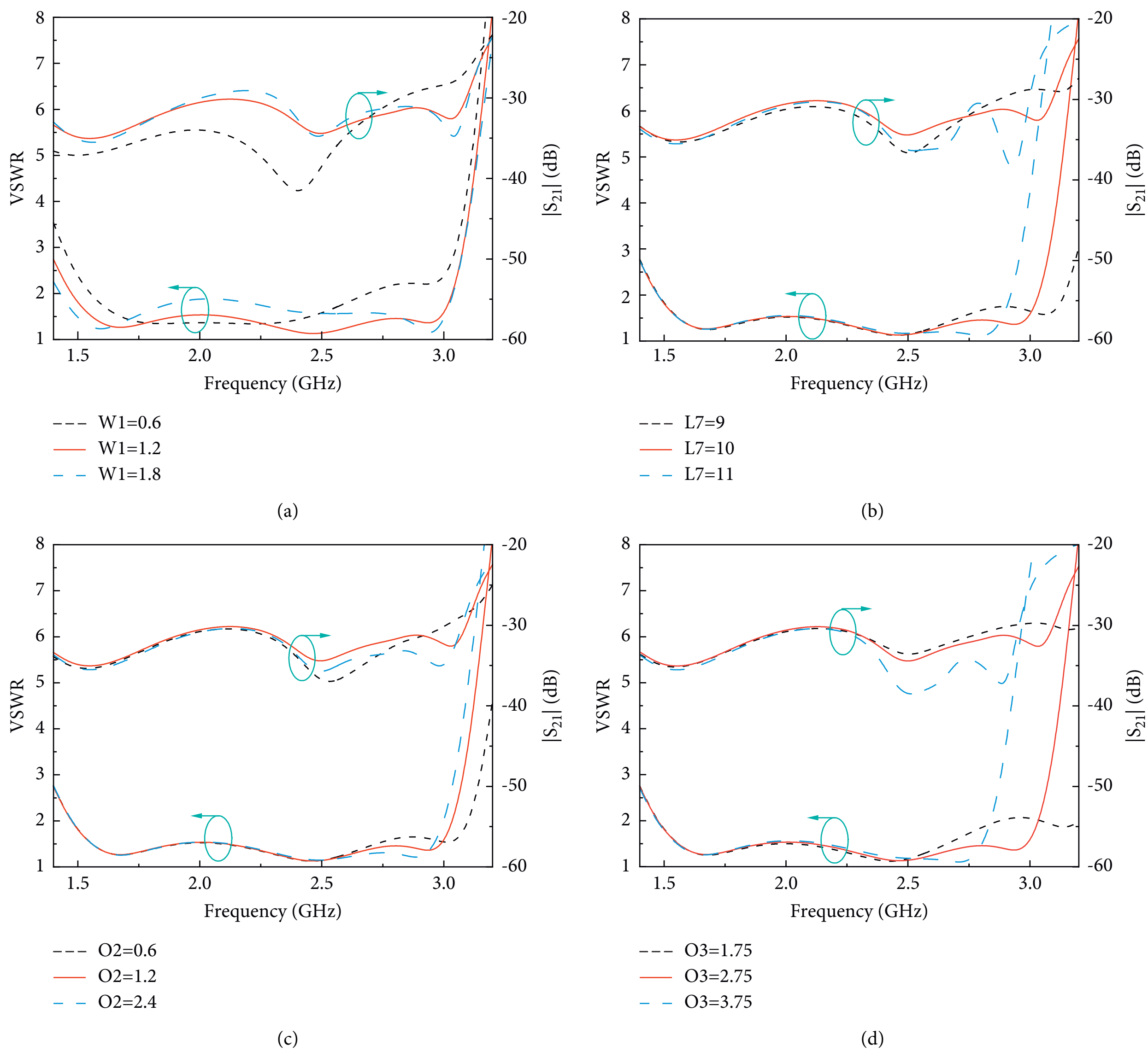

Figure 6: Effects of (a) W1; (b) L7; (c) O2; (d) O3 on VSWR and $|S_{21}|$.

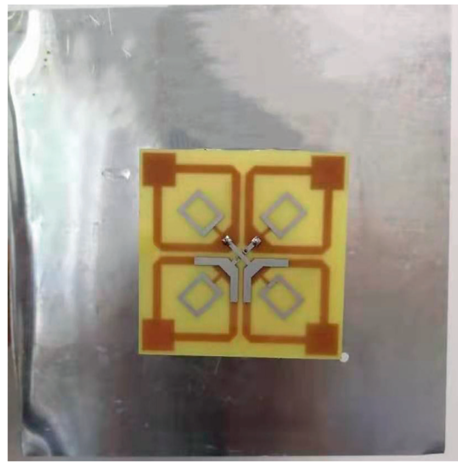

Figure 7: Photograph of the proposed antenna.

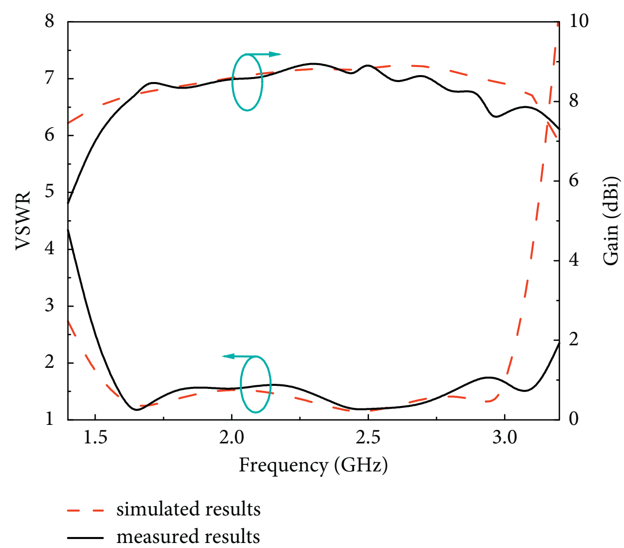

Figure 8: Simulated and measured differential VSWR and gain.

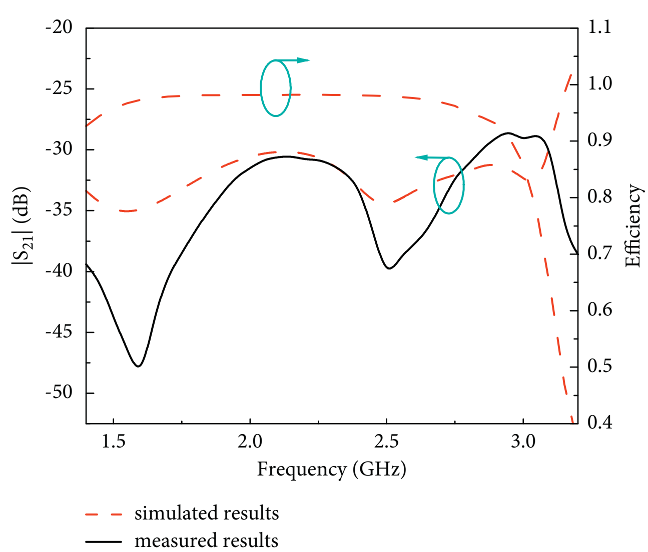

Figure 9: Simulated and measured port-to-port isolation and simulated efficiency of the antenna.

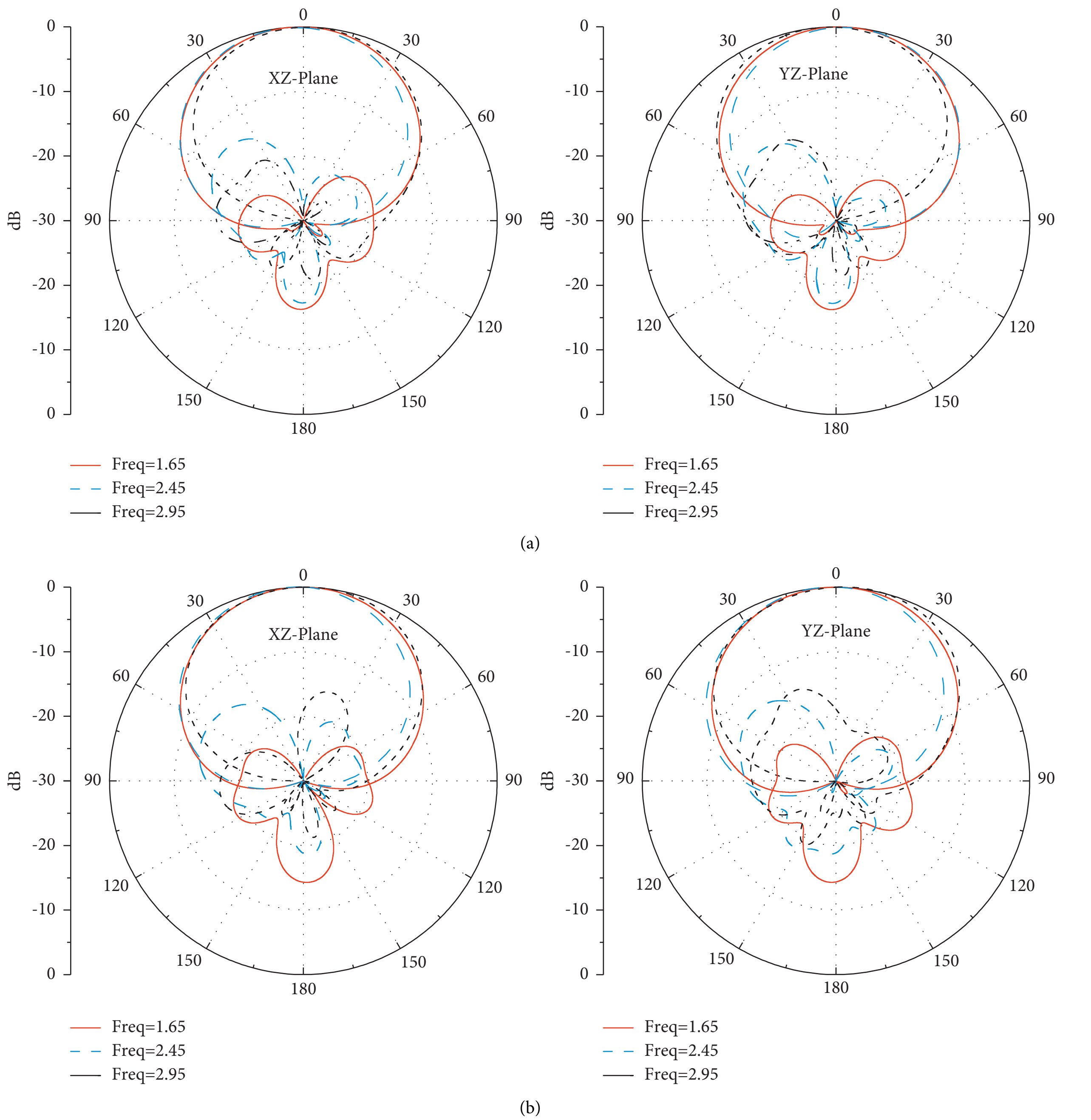

Figure 10: Simulated and measured normalized radiation patterns of the antenna at frequencies 1.65 GHz, 2.45 GHz, and 2.95 GHz. (a) Simulated results. (b) Measured results.

Table 2: Comparison between the proposed antenna and the reported designs.

Ref	Size (λ_0^3)	Impedance bandwidth (%)	Isolation (dB)	Differentially fed/feeding network	Gain (dBi)	HPBW
[1]	$1.08 \times 1.08 \times 0.26$	52.2	>26.3	Yes	~8.5	$66.2^\circ \pm 3.77^\circ$
[2]	$1.12 \times 1.12 \times 0.27$	54.5	>28.5	No	~8.5	$66.2^\circ \pm 3.7^\circ$
[4]	$0.93 \times 0.93 \times 0.23$	30	>25	No	>8	$66.3^\circ \pm 2.9^\circ$
[5]	$0.95 \times 0.95 \times 0.27$	48.2	>30	No	~7.6	$70^\circ \pm 3^\circ$
[6]	$2.07 \times 2.07 \times 0.23$	45	~30	Yes	~8.9	—
[15]	$1.47 \times 0.98 \times 0.26$	45	>30	No	~8.5	65°
[7]	$1.2 \times 1.2 \times 0.27$	52.6	>25.4	Yes	~7.57	$60^\circ \pm 4^\circ$
This work	$0.98 \times 0.98 \times 0.25$	63.7	>30	No	~8	$68^\circ \pm 3^\circ$

4. Conclusions

A wideband dual-polarized multidipole antenna for base station applications has been investigated. Simulated and measured results show that the small rectangle loop dipoles antenna can generate an additional resonance at high frequency. Moreover, the bandwidth has been greatly expanded to 63.7% for VSWR < 1.5. Similarly, the isolation of the antenna is as high as 48 dB, the gain is fluctuating between 6.7 dBi and 8.7 dBi within operating frequency, and the antenna has a stable radiation pattern covering all the frequency bands from 1.55 to 3 GHz. The proposed antenna can be applied in the 2 G/3 G/LTE base stations.

Data Availability

The data used to support the findings of this study are included in the article.

Conflicts of Interest

The authors declare that there are no conflicts of interest regarding the publication of this paper.

Acknowledgments

This work was supported by Key-Area Research and Development Program of Guangdong Province (2020B010170002 and 2019b010145001) and by Science and Technology Program of Guangdong Province (2019A141401005 and 2019A1515012127).

References

[1] D.-L. Wen, D.-Z. Zheng, and Q.-X. Chu, "A wideband differentially fed dual-polarized antenna with stable radiation pattern for base stations," *IEEE Transactions on Antennas and Propagation*, vol. 65, no. 5, pp. 2248–2255, 2017.

[2] D.-Z. Zheng and Q.-X. Chu, "A wideband dual-polarized antenna with two independently controllable resonant modes and its array for base-station applications," *IEEE Antennas and Wireless Propagation Letters*, vol. 16, pp. 2014–2017, 2017.

[3] K. L. Wong, *Compact and Broadband Microstrip Antennas*, Wiley, Hoboken, NJ, USA, 2002.

[4] D.-L. Wen, D.-Z. Zheng, and Q.-X. Chu, "A dual-polarized planar antenna using four folded dipoles and its array for base stations," *IEEE Transactions on Antennas and Propagation*, vol. 64, no. 12, pp. 5536–5542, 2016.

[5] Y. Liu, J. Wang, and S. Gong, "Wideband dual-polarized planar antenna for base stations," *Microwave and Optical Technology Letters*, vol. 57, no. 8, pp. 1948–1952, 2015.

[6] Y. Jin and Z. Du, "Broadband dual-polarized F-probe fed stacked patch antenna for base stations," *IEEE Antennas and Wireless Propagation Letters*, vol. 14, pp. 1121–1124, 2015.

[7] H. Huang, Y. Liu, and S. Gong, "A broadband dual-polarized base station antenna with anti-interference capability," *IEEE Antennas and Wireless Propagation Letters*, vol. 16, pp. 613–616, 2017.

[8] X. J. Lin, Z. M. Xie, and P. S. Zhang, "High isolation dual-polarized patch antenna with hybrid ring feeding," *International Journal of Antennas and Propagation*, vol. 2017, Article ID 6193102, 6 pages, 2017.

[9] L. H. Ye, X. Y. Zhang, Y. Gao, and Q. Xue, "Wideband dual-polarized two-beam antenna array with low sidelobe and grating-lobe levels for base-station applications," *IEEE Transactions on Antennas and Propagation*, vol. 67, no. 8, pp. 5334–5343, 2019.

[10] Y. He, W. Tian, and L. Zhang, "A novel dual-broadband dual-polarized electrical downtilt base station antenna for 2G/3G applications," *IEEE Access*, vol. 5, pp. 15241–15249, 2017.

[11] W. Yang and Y. Pan, "A wideband dual-polarized dipole antenna with folded metallic plates," *IEEE Antennas and Wireless Propagation Letters*, vol. 17, no. 10, pp. 1797–1801, 2018.

[12] D. Q. Yang, H. L. Zeng, Y. B. Wen, M. Zou, and J. Pan, "Design of wideband dual-polarized planar antenna using multimode concept," *International Journal of Antennas and Propagation*, vol. 2016, Article ID 1286398, 10 pages, 2016.

[13] Z. Tang, J. Liu, and Y. Yin, "Enhanced cross-polarization discrimination of wideband differentially fed dual-polarized antenna via a shorting loop," *IEEE Antennas and Wireless Propagation Letters*, vol. 17, no. 8, pp. 1454–1458, 2018.

[14] R. Wu and Q.-X. Chu, "A broadband dual-polarized antenna with chamfers," *Microwave and Optical Technology Letters*, vol. 59, no. 3, pp. 631–635, 2017.

[15] Y. Cui, R. Li, and H. Fu, "A broadband dual-polarized planar antenna for 2G/3G/LTE base stations," *IEEE Transactions on Antennas and Propagation*, vol. 62, no. 9, pp. 4836–4840, 2014.